JOURNAL OF VIROLOGY, Mar. 2000, p. 2714–2720 Vol. 74, No. 6
0022-538X/00/$04.00+0

Role of Hemagglutinin Surface Density in the Initial Stages of Influenza Virus Fusion: Lack of Evidence for Cooperativity

SUSANNE GÜNTHER-AUSBORN,[1]† PIETER SCHOEN,[2]‡ INGRID BARTOLDUS,[1] JAN WILSCHUT,[2]* AND TOON STEGMANN[3]*

Department of Biophysical Chemistry, Biozentrum of the University of Basel, CH 4056 Basel, Switzerland,[1] Institut de Pharmacologie et de Biologie Structurale, CNRS UPR 9062, 31077 Toulouse Cedex, France,[3] and Laboratory of Molecular Virology, Department of Medical Microbiology, University of Groningen, 9713 AV Groningen, The Netherlands[2]

Received 16 August 1999/Accepted 14 December 1999

Membrane fusion mediated by influenza virus hemagglutinin (HA) is believed to proceed via the cooperative action of multiple HA trimers. To determine the minimal number of HA trimers required to trigger fusion, and to assess the importance of cooperativity between these HA trimers, we have generated virosomes containing coreconstituted HAs derived from two strains of virus with different pH dependencies for fusion, X-47 (optimal fusion at pH 5.1; threshold at pH 5.6) and A/Shangdong (optimal fusion at pH 5.6; threshold at pH 6.0), and measured fusion of these virosomes with erythrocyte ghosts by a fluorescence lipid mixing assay. Virosomes with different X-47-to-A/Shangdong HA ratios, at a constant HA-to-lipid ratio, showed comparable ghost-binding activities, and the low-pH-induced conformational change of A/Shangdong HA did not affect the fusion activity of X-47 HA. The initial rate of fusion of these virosomes at pH 5.7 increased directly proportional to the surface density of A/Shangdong HA, and a single A/Shangdong trimer per virosome appeared to suffice to induce fusion. The reciprocal of the lag time before the onset of fusion was directly proportional to the surface density of fusion-competent HA. These results support the notion that there is no cooperativity between HA trimers during influenza virus fusion.

Influenza virus enters its host cell by endocytosis. The low pH inside the endosome triggers conformational changes in the major viral membrane protein, hemagglutinin (HA), leading to fusion of the viral with the endosomal membrane. Besides studies on the structure of HA (8, 40), two different approaches have contributed to making the mechanism of HA-induced fusion the best-understood paradigm for biological membrane fusion. The first involves the fusion of intact virus or reconstituted viral membranes with model membranes (mostly liposomes) or cells, enabling kinetic and quantitative analysis of fusion mediated by HA under physiological conditions. In the second, HA is expressed on the surface of cells, and fusion of these cells with other cells or model membranes may be measured by a variety of methods. Although the latter approach has many advantages, enabling for example mutagenesis of HA and variation of the HA density, the surface of a cell does not have the same curvature as a viral membrane, the density of cell surface-expressed HA is generally much lower than that on virus particles, and, in contrast to the viral membrane, the plasma membrane contains many other proteins. These differences from viral membranes may be important because the HA surface density has been shown to affect fusion kinetics (3, 9, 12, 22), while curvature is an important parameter considered in fusion models (10, 27), and the influence of cellular membrane components has been demonstrated by the effect of neuraminidase treatment on cell-cell fusion (15, 19, 25).

Using cell lines expressing HA, several observations have indicated that the multiple HA trimers are required for fusion and that the interaction between these trimers may be cooperative. Initially, using cell lines expressing HA, Ellens et al. found that 4.4 times more liposomes fused with cells expressing 1.9 times more HA on their surface (15). Later, several different cell lines, expressing HA at different surface densities, were derived from these cells. It was found that they all induced fusion with erythrocytes to the same extent but with different kinetics (12). Fusion in this system is characterized by two kinetic phases: a lag phase after the shift to low pH and a fusion phase. It was found that cooperative interactions between HA trimers took place during the lag phase, but not during fusion, and the number of HA trimers required for fusion was estimated to be at least 3 (12). Using one of these same cell lines, but a different experimental and theoretical approach, others came to the conclusion that six trimers were required for fusion (3) or that fusion was not cooperative at the level of the principal rate-determining step, without excluding possible cooperativity at another step (11).

Here we have investigated the cooperativity of HA-induced fusion and the number of HA trimers minimally required for fusion by analyzing the kinetics of fusion of reconstituted viral membranes (virosomes) with erythrocyte ghosts. To this end, the HAs of two different virus strains, one with optimal fusion at pH 5.7 and the other at pH 5.1, both of the H3 subtype, were coreconstituted into virosomes at various ratios, allowing the activation of a defined number of HAs, at a constant total HA concentration. The results indicate that as little as one HA trimer may trigger fusion, and we do not find evidence for cooperativity.

* Corresponding author. Mailing address for Jan Wilschut: Department of Medical Microbiology, University of Groningen, Ant. Deusinglaan 1, 9713 AV Groningen, The Netherlands. Phone: 31 50 3632733. Fax: 31 50 3632728. E-mail: J.C.Wilschut@med.rug.nl. Mailing address for Toon Stegmann: Institut de Pharmacologie et de Biologie Structurale, CNRS UPR 9062, 205 Route de Narbonne, 31077 Toulouse Cedex, France. Phone: 33 5 61 17 54 63. Fax: 33 5 61 17 59 94. E-mail: stegmann@ipbs.fr.

† Present address: s_ausborn@hotmail.com.

‡ Present address: Haemoprobe BV, 9713 GX Groningen, The Netherlands.

MATERIALS AND METHODS

Materials. *N*-(Lissamine rhodamine B sulfonyl)phosphatidylethanolamine (*N*-Rh-PE) and *N*-(7-nitro-2,1,3-benzoxadiazol-4-yl)phosphatidylethanolamine (*N*-NBD-PE) were purchased from Avanti Polar Lipids (Birmingham, Ala.). Octaethyleneglycol mono-(*n*-dodecyl) ether ($C_{12}E_8$) was obtained from Fluka (Buchs, Switzerland), and 4-chloro-7-nitrofurazan was from Fluka (St. Quentin Fallavier, France). BioBeads SM-2 were from Bio-Rad (Richmond, Calif.). Rhodamine isothiocyanate and Sephadex G-75 were purchased from Sigma (St. Quentin Fallavier, France).

Viruses. The X-47 recombinant strain as well as the A/Shangdong strain of influenza virus (both of the H3 serotype) were propagated in the allantoic cavity of embryonated eggs, purified, handled, and stored as described elsewhere (30). Viral phospholipid phosphate was determined by phosphate analysis (5) after extraction of membrane lipids as described by Folch et al. (16). Protein was determined by the method of Peterson (23).

Preparation of erythrocyte ghosts. Resealed human erythrocyte ghosts were prepared from erythrocyte concentrates obtained from the blood bank of the Kantonsspital (Basel, Switzerland) (blood group A positive) by the method of Steck and Kant (29) with modifications as described by Stegmann et al. (34). Erythrocyte protein concentrations were determined as described above. Ghosts (at a concentration of 1 mg of protein/ml) were stored in the presence of 0.02% NaN_3 at 4°C and used within 3 weeks.

Reconstitution of virus. Reconstitution of influenza virus (either X-47 or A/Shangdong) was carried out as described by Stegmann et al. (35). A concentrated pellet of influenza virus (1 μmol of viral phospholipid) was solubilized in 0.7 ml of 75 mM $C_{12}E_8$ in buffer (145 mM NaCl, 2.5 mM HEPES [pH 7.4]) for 30 min at 4°C. After removal of the ribonucleoprotein complex by centrifugation at 160,000 × *g* for 30 min, the supernatant was added to a dried lipid film composed of *N*-NBD-PE and *N*-Rh-PE and vortexed vigorously. After complete dissolution, the mixture was added to washed BioBeads SM-2 (20 mg of dry beads/70 μl) and shaken at 1,400 rpm in an Eppendorf shaker for 1 h at room temperature. Subsequently, the suspension was added to fresh BioBeads (10 mg/70 μl) and shaking was continued for 10 min under the same conditions. The suspension was loaded on top of a layer of 5% (wt/wt) sucrose in buffer as described above. The centrifuge tube contained a cushion of 40% sucrose in the same buffer. Centrifugation was performed for 90 min with a Beckmann TST 60.4 rotor at 160,000 × *g* and 4°C. Purified virosomes were collected from the interface. Coreconstitutes containing HA from both X-47 and A/Shangdong in different ratios in the same membrane were prepared in a similar manner. The viruses were solubilized separately with $C_{12}E_8$, and different ratios of the HA-containing supernatants were mixed before addition to *N*-NBD-PE and *N*-Rh-PE, removal of detergent, and purification. The amount of *N*-NBD-PE and *N*-Rh-PE in the dried lipid film corresponded to 0.8 mol% each of total phospholipid in the reconstituted membrane.

Fluorescence labeling of HA. To label HA with NBD, whole virus (5 mg of protein) was resuspended in 100 mM $NaHCO_3$ buffer (500 μl), 25 μl of a 10-mg/ml solution of 4-chloro-7-nitrofurazan in dry dimethyl sulfoxide was added stepwise, and the mixture was left to incubate for 41 h in the dark at 0°C with agitation. To label HA with rhodamine, 25 μl of a 10-mg/ml solution of rhodamine isothiocyanate was added stepwise to whole virus, resuspended in 100 mM $NaHCO_3$ buffer (500 μl), and incubated for 8 h in the dark at 0°C with agitation. After labeling, excess reactive probe was consumed by adding an aliquot of Tris-HCl (100 mM, pH 8) and subsequently removed by gel filtration on a 10-ml Sephadex G-75 column. Fluorescent virus was concentrated by ultracentrifugation, and the viral membranes were reconstituted as described above. Because rhodamine isothiocyanate and 4-chloro-7-nitrofurazan are amine-reactive reagents, they potentially label viral amino lipids as well. Although we found it difficult to analyze this with great precision, traces of rhodamine- but not NBD-labeled lipids were seen on thin-layer chromatography plates, but more than 50% of the virus-associated NBD label was found associated with viral membrane proteins (results not shown) and most of the remainder was found associated with viral nonmembrane proteins.

Fusion measurements. Fusion between labeled virosomes and unlabeled erythrocyte ghosts was measured by resonance energy transfer (37). Fluorescence measurements were performed on a Schoeffel RRS 1000 fluorimeter at excitation and emission wavelengths of 465 and 530 nm, respectively. A 515-nm long-pass filter was placed between the cuvette and the emission monochromator. All measurements were carried out with continuous stirring in 2 ml of 135 mM NaCl–15 mM sodium citrate–10 mM morpholineethanesulfonic acid–5 mM HEPES buffer at the pH and temperatures indicated. The initial rates of fusion (percent fluorescence increase per minute) were calculated after calibration of the fluorescence scale as described elsewhere (17).

Binding assays. To measure the binding of fluorescently labeled virosomes to unlabeled ghosts, virosomes were incubated with ghosts at 0°C for 15 min and then the mixture was centrifuged for 3 min at 16,000 × *g*. Under these circumstances, the ghosts and ghost-associated virosomes are pelleted whereas free virosomes remain in the supernatants. After the addition of Triton X-100 to pellets and supernatants, the fluorescence of *N*-NBD-PE was determined, and the percentage of binding was calculated as follows: $100 \times [F_{\text{Pellet}} - A\,(F_{\text{Pellet}} + F_{\text{Supernatant}})]/(F_{\text{Pellet}} + F_{\text{Supernatant}})$. In this equation, A represents the fraction of virosomes pelleted in the absence of ghosts and F stands for fluorescence.

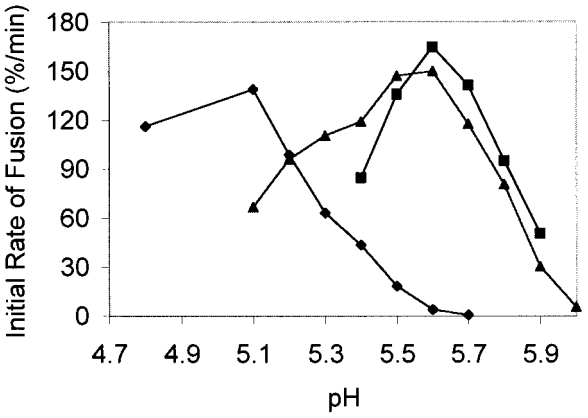

FIG. 1. pH dependencies of the initial rate of fusion of virosomes containing X-47 HA (◆), A/Shangdong HA (■), or a 1:1 mixture of both (▲). Erythrocyte ghosts were equilibrated in fusion buffer at the indicated pH for 3 min, at 37°C, before the injection of *N*-NBD-PE- and *N*-Rh-PE-labeled virosomes into the cuvette. Fusion was measured as described in Materials and Methods. Final concentrations were 50 μg of ghost protein per ml and 5 μM virosomes (phospholipid phosphate). The results shown were obtained with the same batch of ghosts and virosomes, and the fusion rates are representative of repeated experiments, although the rates may vary between ghost preparations.

RESULTS

Virosomes containing HA from either X-47 or A/Shangdong virus have different pH dependencies of the initial rate of fusion, can be coreconstituted into one membrane, and bind target membranes to similar extents. In order to determine the number of HA trimers required for fusion, and the cooperativity of their interactions, we intended to study the kinetics of fusion as a function of the HA surface density in a well-defined model system in which reconstituted viral envelopes (virosomes) fuse with a biological target membrane (erythrocyte ghosts). In this system, the HA surface density is easily controlled by the protein-to-lipid ratio of the mixture from which the liposomes are prepared. Initial studies showed, however, that under these conditions the kinetics of fusion were influenced by the efficiency of virosome-target membrane binding as mediated by HA-receptor interactions. We circumvented this problem by using hybrid virosomes, prepared from two strains of virus with different pH dependence such that at an intermediate pH, the HAs of only one strain would be active, while the others would not undergo a low pH-dependent conformational change. These hybrid virosomes would enable us to manipulate the surface density of fusion-active HA, at a constant protein-to-lipid ratio, so that HA-target membrane binding would be independent of fusion-competent HA surface density. To test the feasibility of this approach, virosomes containing either A/Shangdong HA or X-47 HA alone were first prepared. Virus was solubilized with the detergent $C_{12}E_8$, and the viral ribonucleoprotein complex was pelleted by ultracentrifugation. The supernatant, containing the viral membrane proteins and lipids, was added to a dry lipid film containing the fluorescent probes *N*-NBD-PE and *N*-Rh-PE, and the membranes were reconstituted by removal of the detergent by BioBeads (6, 35). After purification of the resulting fluorescently labeled virosomes on a sucrose gradient, fusion with erythrocyte ghosts was measured by a resonance energy transfer assay (37). The pH dependencies of the membrane fusion rate induced by the HAs of A/Shangdong and X-47 virosomes were found to be different (Fig. 1). Reconstituted X-47 HA has optimal activity at pH 5.1 and a threshold pH for fusion of 5.5, closely resembling the pH dependence of the native virus (32).

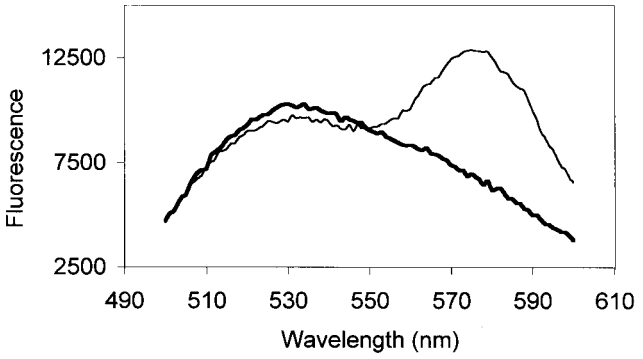

FIG. 2. Resonance energy transfer from NBD-labeled X-47 to rhodamine-labeled A/Shangdong HAs. Both HAs were reconstituted together, at a 1:1 ratio (thin line), or the HAs were reconstituted separately and the resulting membranes were mixed 1:1 after reconstitution (bold line). Data are for 10 nmol of virosomes in 2 ml of buffer at pH 7.4, 0°C. HAs were labeled and reconstituted as described in Materials and Methods.

A/Shangdong HA showed an optimum at pH 5.6 with a threshold at pH 6.0. Therefore, at pH 5.7, A/Shangdong HA is fusion competent while HA from X-47 is not active.

To demonstrate the coreconstitution of X-47 HA with A/Shangdong HA in the same membrane, we labeled A/Shangdong HA with rhodamine and X-47 HA with NBD, as described in Materials and Methods. Virosomes were then produced from either NBD–X-47 or rhodamine-A/Shangdong HA alone or from a 1:1 mixture of both HAs. After excitation at 460 nm, the excitation wavelength of NBD, we found clear evidence for resonance energy transfer from NBD-HA to rhodamine-HA with the coreconstitutes but not with a 1:1 mixture of virosomes containing only NBD-HA or rhodamine-HA (Fig. 2). These data indicate that after coreconstitution, the two different types of HA were present in the same membrane. The efficiency of energy transfer was calculated as described by Struck et al. (37), from the fluorescence of NBD from virosomes containing both HAs before and after addition of detergent to the sample. The observed efficiency, 0.31, is compatible with an NBD fluorophore concentration of around 0.2 mol% with respect to the membrane lipids (37). Given 100,000 lipids per virosome, this means that, on the average, an NBD-carrying X-47 HA trimer is separated by 456 lipids from a rhodamine-linked A-Shangdong HA as measured by resonance energy transfer. Given that there are around 500 HA trimers per virosome (35), or 1 X-47 HA per 400 lipids, these data clearly indicate that HAs were reconstituted individually in the membrane. Similar results were obtained at several other ratios of the two types of HA.

In particular, HA present on the plasma membrane of cells but also viral HA has been shown to reside partly in rafts, specialized lipid domains that potentially contain multiple HA proteins and are not soluble in some detergents at low temperatures (26, 28). If the X-47 and A/Shangdong HAs were present on rafts during reconstitution, we would not be able to reconstitute individual HA trimers as desired. Since HA present on rafts, in contrast to HA trimers individualized in detergents, has been shown to be pelleted by 30 min of centrifugation at 120,000 × *g* (18), we subjected the HA-containing supernatant used for reconstitution to such centrifugation. Less than 1% of the HA was found to be pelleted, indicating that HA is not present on rafts during reconstitution and that we are reconstituting individual trimers. Moreover, complete relief of energy transfer was obtained after detergent lysis of hybrid virosomes containing both HAs (data not shown), showing that during reconstitution, monomers of the two HAs are not exchanged between trimers.

Subsequently, the pH dependence of coreconstitute fusion was determined. The X-47 and A/Shangdong strains of virus were solubilized with $C_{12}E_8$, and after ultracentrifugation the HA-containing supernatants were mixed in the presence of the two fluorescent phospholipid analogues, *N*-NBD-PE and *N*-Rh-PE. After removal of $C_{12}E_8$ and purification of the virosomes as described in Materials and Methods, fusion with erythrocyte ghosts was measured as described above. The initial rates of fusion as a function of pH are shown in Fig. 1. The profile shows that at the pH values at which X-47 is not active, hybrid virosomes show a pronounced fusion activity which closely follows the profile of A/Shangdong virosomes alone. Moreover, below pH 5.4, A/Shangdong HA becomes inactivated, but the fusion activity of hybrid virosomes remains. Taken together, these data and those of Fig. 2 demonstrate that the two types of HA are present in the same membrane and that these HAs are active.

Coreconstitution of the two different HAs in the same membrane at different ratios would allow the activation of the fusogenic capacity of different concentrations of HA, while keeping the total concentration of HA, and thus other properties, such as HA-receptor binding, constant. This hypothesis was validated by determining binding of virosomes, containing different ratios of X-47 to A/Shangdong HAs, to erythrocyte ghosts at neutral pH. Under these conditions, binding is caused solely by receptor-ligand interactions between the HA1 subunit and sialic acid. After binding of virosomes, containing 0, 10, 20, or 100% HA from X-47 supplemented with A/Shangdong HA, to ghosts for 15 min at 0°C and pH 7.4, ghost-associated virosomes were separated from free virosomes by centrifugation, and the fluorescence of the ghost pellet was determined. It was found that these different virosomes bound to erythrocyte ghosts to the same extent (Fig. 3).

Low pH-induced inactivation of A/Shangdong HA does not affect the fusion induced by HA from X-47 coreconstituted in the same membrane. As a result of the low pH-induced conformational change, the fusion capacity of HAs of the H3 serotype is rapidly inactivated in the absence of target mem-

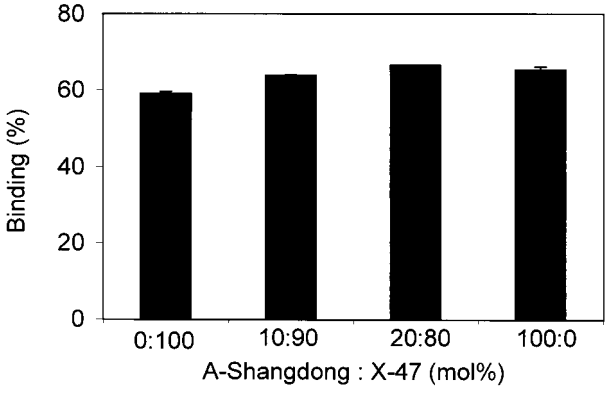

FIG. 3. Binding of coreconstitutes containing different ratios of HA from X-47 and A/Shangdong to ghosts at neutral pH. Ten nanomoles of fluorescently labeled virosomes was incubated with ghosts (100 μg of protein) in 2 ml of buffer at pH 7.4 and 0°C for 15 min, and then the mixture was centrifuged for 3 min at 16,000 × *g*. Binding was determined in duplicate measurements as described in Materials and Methods. Error bars are ±1 standard deviation. The results shown are representative of repeated experiments and were obtained with the same batch of ghosts and virosomes. The absolute amount of binding may vary between ghost preparations.

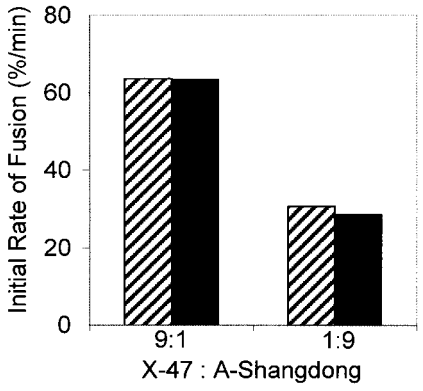

FIG. 4. Effect of inactivation of HA from A/Shangdong at pH 5.6 on X-47-mediated fusion at pH 5.1. Coreconstitutes containing HAs from both strains of virus were prepared at a 9:1 or 1:9 (X-47-to-A/Shangdong) molar ratio as described in Materials and Methods. Ten nanomoles of virosomes was preincubated in a small volume of buffer at pH 5.6 in the absence of target membranes for 15 min at 37°C. Subsequently, the rate of fusion was measured at pH 5.1 and 37°C (dark bars) and compared to the initial rate of the corresponding untreated coreconstitutes measured under the same conditions (hatched bars).

branes (34). In order to investigate whether the conformational change induced in the A/Shangdong HA at its optimum pH, 5.6, would trigger, or alternatively prevent, the conformational change in X-47 HA, virosomes containing either X47 or A/Shangdong HA alone, or X-47 and A/Shangdong HAs in the same membrane at a 1:9 or a 9:1 molar ratio, were prepared. First, virosomes containing only one type of HA were incubated at the absence of target membranes at pH 5.6, 37°C, for 15 min. Subsequently, these virosomes were added to erythrocyte ghosts and fusion was measured at the specific pH optimum for fusion. HA from A/Shangdong did not show any remaining fusion activity towards ghosts, indicating complete inactivation under these conditions (data not shown). However, X-47 HA fusion activity was not affected. Different preparations of virosomes containing both HAs (at a 1:9 or 9:1 molar ratio) in the same membrane were then preincubated under the same conditions in order to inactivate A/Shangdong HA. Subsequently, fusion with ghosts was measured at pH 5.1. As shown in Fig. 4, the low-pH preincubation did not affect the fusion kinetics of these virosomes (in comparison to that of untreated virosomes). These data show that when one type of HA undergoes a complete conformational change, this does not induce a conformational change that leads to activation and subsequent inactivation in the other type. Even if HA from X-47 is surrounded by a large number of fusion-inactive HAs (up to 90% in this case), it is not affected and keeps its full fusion competence.

Effect of HA surface density on initial rate and lag time of fusion. Using the coreconstitution procedure described above, virosomes containing 0 to 100 mol% A/Shangdong HA, supplemented with X-47 HA to 100 mol%, were prepared and the initial rates (Fig. 5A) and final level (Fig. 5B) of fusion at pH 5.7, 37°C, were measured as described in Materials and Methods. These rates were obtained after injection of labeled virosomes into a cuvette containing a large excess of ghosts at low pH. Since fusion (membrane merger) is always preceded by binding of the two membranes, we validated that the actual merging, and not binding, was rate limiting under these circumstances by comparing the fusion kinetics obtained by this method with the fusion kinetics obtained after binding of virosomes (several different ratios of A/Shangdong to X-47 HA) and ghosts at pH 7.4, 0°C, for 5 min prior to acidification. The

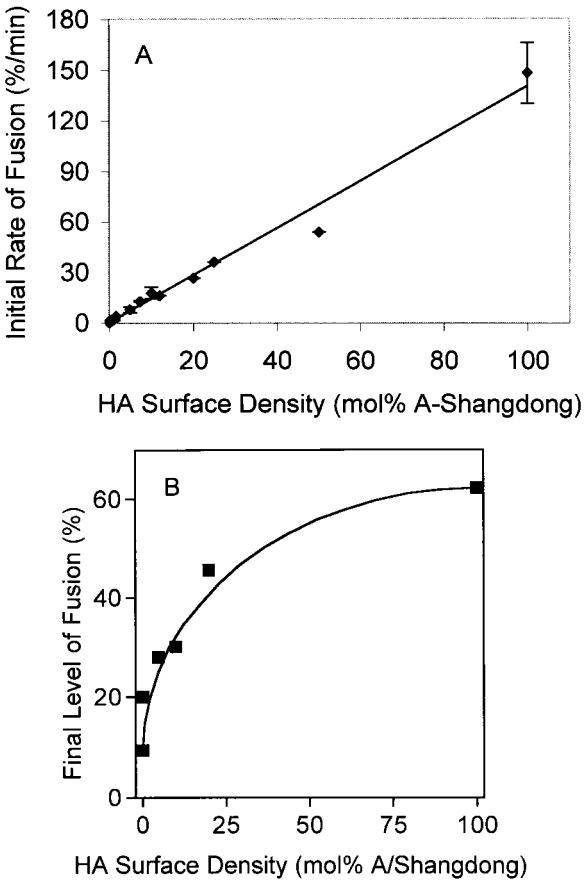

FIG. 5. Effect of HA surface density on the initial rate and final level of fusion at pH 5.7 and 37°C. Fusion of coreconstitutes containing different ratios of A/Shangdong to X-47 HAs with ghosts was measured at pH 5.7 under conditions described in the legend to Fig. 1. (A) Combination of results obtained in several independent experiments (four preparations of ghosts and virosomes; 34 fusion measurements). Error bars are ±1 standard deviation; where no error bars are visible, they are smaller than the drawn data point. Reconstitutes containing X-47 HA alone also caused a perceptible fluorescence increase at this pH under these circumstances, at a rate of 0.2 to 0.3%/min. However, considering that this is less than one-third the fusion rate at the lowest concentration of A/Shangdong (0.1 mol%) using the coreconstitutes, or less than one-fifth the rate at the next lowest concentration (0.25 mol%), no corrections were made to account for this residual X-47 activity. (B) Final levels of fusion.

measured fusion kinetics closely matched those reported in Fig. 5A, indicating that under the conditions of this study, membrane merger, and not virosome-ghost binding, is rate limiting.

The initial rates of fusion increased with the concentration of fusion-competent A/Shangdong HAs in the virosomal membrane. The linear relationship between the rate of fusion and the concentration of active HA indicates that the reaction is first order with respect to active HA, which implies a lack of cooperativity between HA trimers. Efficient fusion occurred at a concentration of A/Shangdong HA as low as 0.1 mol%. Assuming that there are about 500 HA trimers per virosome, this concentration would correspond to an average of 0.5 fusion-competent trimer per virosome.

Lag times preceding fusion were determined at pH 5.7 and 15°C. At this temperature, the time interval between exposure to low pH and the onset of fusion is increased relative to those at 37°C (36), making the measurement of lag times more reliable. As shown in Fig. 6A, the lag time increased with decreas-

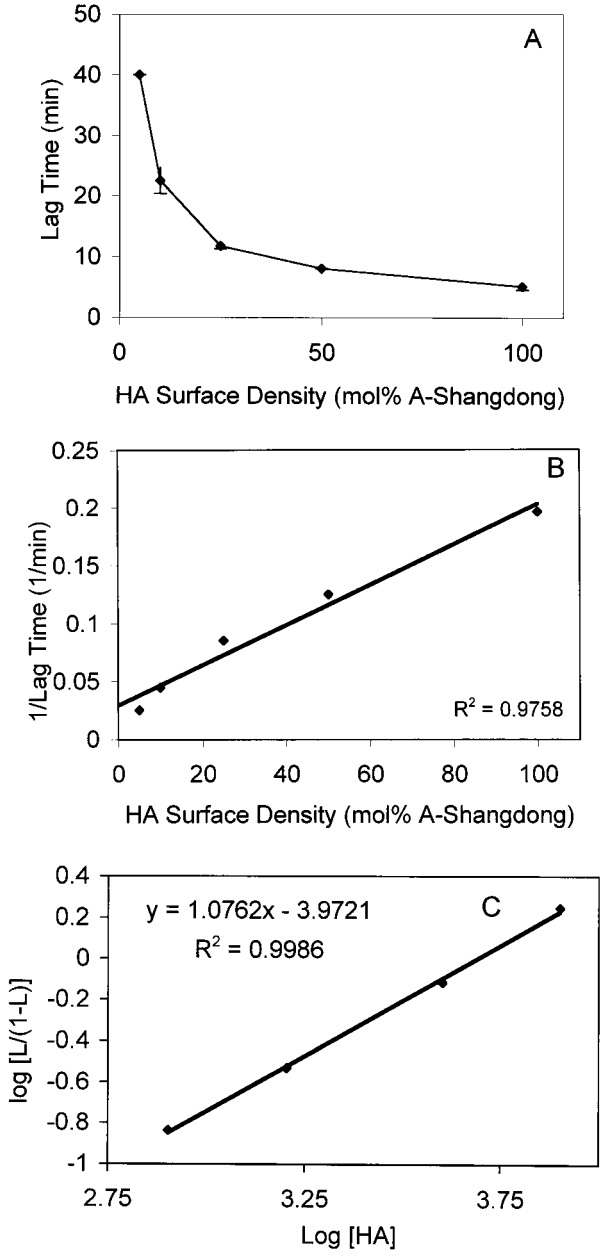

FIG. 6. Effect of HA surface density on the lag phase at pH 5.7 and 15°C. Coreconstitutes containing increasing numbers of fusion-active HA were preincubated for 15 min with erythrocyte ghosts on ice at neutral pH and injected into a cuvette at pH 5.7 and 15°C, and the fluorescence increase was monitored. The lag time was determined as the time between the onset of fusion and the maximal increase in fluorescence (defined as tangent to the curve, where fusion rate is maximal) (as outlined in references 1, 21, and 31). Final concentrations were 50 μg of ghost protein/ml and 5 μM virosomes (phospholipid phosphate). (A) Lag time versus moles percent A/Shangdong. Error bars are ±1 standard deviation. (B) 1/lag time versus moles percent A/Shangdong. (C) Hill-like plot according to Danieli et al. (12). The data from Fig. 6A were transformed as follows. A 1/lag value at saturation was first determined from the three highest data points by plotting 1/lag versus 1/HA density (expressed as trimers per square micrometer) and extrapolating to infinite HA density. The other 1/lag values were then divided by this value, yielding L. Log $[L/(1 - L)]$ was then plotted against log [HA]. As the observed lag at the highest data point (100% Shangdong) was slightly (1.5%) longer than the extrapolated lag at saturation, a real value of log $[L/(1 - L)]$ could not be obtained for this point.

ing concentrations of fusion-competent A/Shangdong HA. Since the lag time is generally thought to represent a process that must be finished either completely or to a defined extent before the membrane merger takes place, these data were further analyzed by plotting the reciprocal lag time versus the active HA concentration (Fig. 6B). A linear relationship was obtained, in contrast to the sigmoidal relationship between these two parameters that was found by Danieli et al. (12). Our data suggest that there also is no cooperative interaction between HA trimers at the level of the lag phase.

DISCUSSION

Following suggestions that influenza virus fusion may be initiated by a fusion complex made of several HA trimers and may thus depend on cooperative interactions between these trimers (2, 4, 13, 36, 39), several groups have addressed this question by using HA expressed on the plasma membrane of cells. Either different cell lines expressing a range of HA concentrations (12, 14) or cell lines treated with reagents that allowed the activation of a fraction of the HA were used (11). Fusion of these cells with liposomes, erythrocytes, or erythrocyte ghosts was studied, and the extent or initial rate of fusion or the lag time before the onset of fusion was measured. Cells expressing HA differ from the viral membrane in several important respects such as HA surface density, membrane curvature, and the presence of proteins other than HA on the cellular membrane. To circumvent these problems, we have taken a different approach. Solubilization of influenza virus with the nonionic detergent $C_{12}E_8$, followed by removal of the detergent using BioBeads, yields reconstituted viral membranes (virosomes) which have essentially the same size (and therefore membrane curvature) and membrane composition as the native virus, an HA surface density which is in the same range as that of the virus, and the same characteristics (such as pH dependence) of fusion as the virus (7, 35). We used this protocol to functionally coreconstitute in the same membrane HAs from two different strains of virus, X-47 and A/Shangdong, which have different fusion rate pH dependencies, allowing the selective activation of A/Shangdong HA, while X-47 HA remains in its neutral pH form. Thus, the HA-to-lipid ratio at different X-47-to-A/Shangdong HA ratios remained constant, and properties like target membrane binding (Fig. 3) were identical for all virosome preparations. Fusion experiments carried out before and after inactivation of A/Shangdong HA at pH 5.7 revealed that X-47 HA, even in the presence of a large number of inactivated HAs, remains in its active form and becomes fully fusion competent only upon acidification to the appropriate pH (Fig. 4). Several mechanisms have been suggested for HA inactivation, for example, insertion of the fusion peptide into the viral instead of the target membrane, making it permanently unavailable for fusion; there is some evidence for this from photolabeling experiments (38). It was also suggested, on the basis of the disorderly arrangement of HA spikes seen by electron microscopy, that lateral aggregation of HA trimers (potentially involving the exposed fusion peptides) could inactivate HA (33). Our present observation that the occurrence of the conformational change in one type of HA, as assessed by fusion inactivation, does not affect the ability of the other type of HA in the same membrane to independently undergo the conformational change, implies that the measured rates (Fig. 5A) and lag times (Fig. 6) of fusion with different ratios of the two types of HA at a constant total HA/lipid ratio are indeed exclusively dependent on the surface density of fusion-competent HA. We can therefore conclude that, at the HA surface density and membrane cur-

vature typical of virus, since both the initial rate of fusion and the reciprocal lag time are linearly dependent on the surface density of fusion-competent HA, there appears to be no evidence for a cooperative interaction between HA trimers.

Our results concerning the initial rate of fusion seem to corroborate the similar conclusions based on experiments involving a number of different cell lines, expressing HA at densities of up to 79% of that of the viral membrane (12). In these studies, the initial rate of fusion exhibited a Michaelis-Menten type of dependence on the HA concentration, which differs from the data shown here in the sense that a saturation of the fusion kinetics was observed at an HA trimer concentration above $3.5 \times 10^3/\mu m^2$, whereas we did not see saturation. Assuming that there are 500 HA trimers per virion (20), and that virus particles are 100 nm in diameter, the HA density used here would be 16×10^3 HA trimers/μm^2. We have previously found that, after $C_{12}E_8$ reconstitution, the HA/lipid ratio in the reconstitute is identical to that of the viral membrane but trimers are present on both sides of the membrane (35). But, even if this is taken into account, the range of densities that Danieli et al. (12) investigated is quite comparable to ours. As suggested by Danieli et al. (12), saturation may thus reflect inherent limitations of the cell-cell fusion assay such as arriving at a saturation density of the number of fusion pores in the area of cell-cell contact or the rate of fluorescent lipid migration into the membrane of the HA-expressing cell. Our studies do not allow us to completely exclude an influence of the HA subtype; the HAs of A/Shangdong and X-47 are of the H3 subtype, whereas the HA used by Danieli et al. is of the H2 subtype, but we think it is unlikely that such basic properties of the fusion mechanism would be different between subtypes.

A lack of cooperativity is supported by the observed efficient triggering of fusion by A/Shangdong HA present at a concentration of 0.1 mol% (Fig. 5A). Assuming 500 HA trimers per virosome, two-thirds of which are on the outside, a Poisson distribution of trimers among the virosomes, and that every single A/Shangdong trimer is activated at the pH of the experiment, 23.7% would have just one A/Shangdong trimer or 28.3% of these virosomes would have one or more active HA trimers. The final level of fluorescence increase obtained with this preparation was about 9.6% after 30 min (Fig. 5B). Although the threshold pH of X-47-induced fusion is mostly reported to be around pH 5.5, under the conditions of the experiment (large excess of target membranes), virosomes containing only X-47 HA (0 mol% A/Shangdong) also gave rise to some fluorescence increase, albeit slowly, reaching 2.8% after 30 min. Therefore, 6.8% fusion can be ascribed to the 28.3% of virosomes that contain one or more A/Shangdong trimers on the external leaflet of the membrane, indicating that one in four of these virosomes is fusion active at these extremely low surface densities of A/Shangdong HA. This is a very significant fraction considering that at high HA densities one in two virosomes fuse (Fig. 5B). Again assuming a Poisson distribution, at 0.1 mol% A/Shangdong HA, 3.9% of the virosomes would have two trimers on the outside and only 0.43% would have three. Although we cannot rigorously exclude the possibility that a small fraction of the virosomes contains all of the fusion-active HA, at the next-lowest concentration of A/Shangdong tested, 0.25 mol%, which corresponds to 56.3% having one or more trimers on the outside of every virosome, fusion already reached 20% (Fig. 5B), i.e., one in three virosomes were active. This result argues in favor of a homogeneous, random distribution of fusion-competent trimers among the virosomes, even at low surface densities. Therefore, our present observations of significant fusion in the case where 28.3% of the virosomes have one or more trimers on the outside support the notion that a single trimer suffices to induce fusion.

Fusion of influenza virus with cells or liposomes, or fusion of HA-expressing cells with cells, is preceded by a lag phase, which depends on temperature and pH, resulting in a sigmoidal appearance of the progress of fusion in time (11, 12, 21, 22, 24, 25, 36). Generally, such a sigmoidal curve is interpreted to mean that one or more processes have to be completed, or must progress to a certain point, before fusion can take place. For influenza-virus induced fusion, it is clear that the lag occurs largely after the low pH-induced conformational change in HA (36); however, the exact processes taking place during the lag phase have never been resolved. In light of the view that fusion requires the formation of a fusion complex involving multiple HA trimers, it has frequently been suggested that the lag time would correspond to the time needed to assemble the complex, a process which might be cooperative or not.

Since the nature of the lag time is unclear, and kinetic data on the changes that might take place during this period are lacking, the method of analysis of lag time data is not obvious. If it represents the end point of a reaction, its rate is probably most reasonably approximated by 1 divided by lag time, which would imply a first-order dependence of the lag on HA concentration and, therefore, no cooperativity. We have used this analysis (Fig. 6B), and it appears to adequately describe our data. Others have suggested that the data be analyzed by plotting log (1/lag) against log (concentration of active trimers) and argued that if the slope of this were 1, it would mean that aggregation of HA trimers to form a fusion complex would not be cooperative, without precluding cooperativity at other levels (11). If we apply this type of analysis to our data, we find a reasonably straight line ($r^2 = 0.996$) but with a slope of 0.68. However, others have presented lag time data in the form of a Hill plot (12), necessitating several assumptions and adaptations, since Hill plots were developed for receptor-ligand binding. If we apply this type of analysis, in the form suggested by Danieli et al. (12), assuming as they did that 100% active HA corresponds to saturation, we obtain a Hill constant of 1.07 (Fig. 6C) ($r^2 = 0.999$), in agreement with the linear relationship between the reciprocal lag time and HA surface density shown in Fig. 6B, thus arguing in favor of the involvement of individual, instead of multiple, HA trimers. Therefore, we conclude that our present results, taken together, do not provide evidence for a cooperative interaction between trimers in membrane fusion mediated by the influenza virus HA.

ACKNOWLEDGMENTS

This study was supported by grant 3100-042953.95/1 from the Swiss National Science Foundation, the Région Midi-Pyrenées, the SIDACTION, and the Fondation pour la Recherche Médicale (to T.S.), by The Netherlands Organization for Scientific Research (NWO) under the auspices of the Chemical Foundation (CW) and the Technology Foundation (STW), and by INEX Pharmaceuticals Co. (Burnaby, British Columbia, Canada).

REFERENCES

1. **Bentz, J.** 1992. Intermediates and kinetics of membrane fusion. Biophys. J. **63:**448–459.
2. **Bentz, J., H. Ellens, and D. Alford.** 1990. An architecture for the fusion site of influenza hemagglutinin. FEBS Lett. **276:**1–5.
3. **Blumenthal, R., D. Sarkar, S. Durell, D. E. Howard, and S. E. Morris.** 1996. Dilation of the influenza hemagglutinin fusion pore revealed by the kinetics of individual cell-cell fusion events. J. Cell Biol. **135:**63–71.
4. **Blumenthal, R., C. Schoch, A. Puri, and M. J. Clague.** 1991. A dissection of steps leading to viral envelope-mediated membrane fusion. Ann. N. Y. Acad. Sci. **635:**285–296.
5. **Böttcher, C. J. F., C. M. Van Gent, and C. Fries.** 1961. A rapid and sensitive

sub-micro phosphorous determination. Anal. Chim. Acta **24:**203–204.
6. **Bron, R., A. Ortiz, J. Dijkstra, T. Stegmann, and J. Wilschut.** 1993. Preparation, properties and applications of reconstituted influenza virus envelopes. Methods Enzymol. **220:**313–331.
7. **Bron, R., A. Ortiz, and J. Wilschut.** 1994. Cellular cytoplasmic delivery of a polypeptide toxin by reconstituted influenza virus envelopes (virosomes). Biochemistry **33:**9110–9117.
8. **Bullough, P. A., F. M. Hughson, J. J. Skehel, and D. C. Wiley.** 1994. Structure of influenza haemagglutinin at the pH of membrane fusion. Nature **371:**37–43.
9. **Chernomordik, L. V., E. Leikina, V. Frolov, P. Bronk, and J. Zimmerberg.** 1998. The pathway of membrane fusion catalyzed by influenza hemagglutinin: restriction of lipids, hemifusion, and lipidic fusion pore formation. J. Cell Biol. **140:**1369–1382.
10. **Chernomordik, L. V., and J. Zimmerberg.** 1995. Bending membranes to the task: structural intermediates in bilayer fusion. Curr. Opin. Struct. Biol. **5:**541–547.
11. **Clague, M. J., C. Schoch, and R. Blumenthal.** 1991. Delay time for influenza hemagglutinin-induced membrane fusion depends on the hemagglutinin surface density. J. Virol. **65:**2402–2407.
12. **Danieli, T., S. L. Pelletier, Y. I. Henis, and J. M. White.** 1996. Membrane fusion mediated by the influenza hemagglutinin requires the concerted action of at least three hemagglutinin trimers. J. Cell Biol. **133:**559–569.
13. **Doms, R. W., and A. Helenius.** 1986. Quaternary structure of influenza virus hemagglutinin after acid treatment. J. Virol. **60:**833–839.
14. **Ellens, H., J. Bentz, D. Mason, F. Zhang, and J. White.** 1990. Fusion of influenza hemagglutinin-expressing fibroblasts with glycophorin-bearing liposomes: role of hemagglutinin surface density. Biochemistry **29:**9697–9707.
15. **Ellens, H., S. Doxsey, J. S. Glenn, and J. M. White.** 1989. Delivery of macromolecules into cells expressing a viral membrane fusion protein. Methods Cell Biol. **31:**155–178.
16. **Folch, J., M. Lees, and G. H. Sloane-Stanley.** 1957. A simple method for the isolation and purification of total lipids from animal tissues. J. Biol. Chem. **226:**497–509.
17. **Günther-Ausborn, S., A. Praetor, and T. Stegmann.** 1995. Inhibition of influenza-induced membrane fusion by lysophosphatidylcholine. J. Biol. Chem. **270:**29279–29285.
18. **Keller, P., and K. Simons.** 1998. Cholesterol is required for surface transport of influenza virus hemagglutinin. J. Cell Biol. **140:**1357–1367.
19. **Kemble, G. W., T. Danieli, and J. M. White.** 1994. Lipid-anchored influenza hemagglutinin promotes hemifusion, not complete fusion. Cell **76:**383–391.
20. **Lamb, R. A., and R. M. Krug.** 1996. Orthomyxoviridae, p. 1091–1152. *In* B. N. Fields, D. M. Knipe, and P. M. Howley (ed.), Fundamental virology. Lippincott-Raven, Philadelphia, Pa.
21. **Ludwig, K., T. Korte, and A. Herrman.** 1995. Analysis of delay times of hemagglutinin-mediated fusion between influenza virus and cell membranes. Eur. Biophys. J. **24:**55–64.
22. **Morris, S. J., D. P. Sarkar, J. M. White, and R. Blumenthal.** 1989. Kinetics of pH-dependent fusion between 3T3 fibroblasts expressing influenza hemagglutinin and red blood cells. Measurement by dequenching of fluorescence. J. Biol. Chem. **264:**3972–3978.
23. **Peterson, G. L.** 1977. A simplification of the protein assay method of Lowry et al. which is more generally applicable. Anal. Biochem. **83:**346–356.
24. **Ramalho-Santos, J., S. Nir, N. Düzgünes, A. Pato de Carvalho, and M. da Conceição Pedroso de Lima.** 1993. A common mechanism for influenza virus fusion activity and inactivation. Biochemistry **32:**2771–2779.
25. **Sarkar, D. P., S. J. Morris, O. Eidelman, J. Zimmerberg, and R. Blumenthal.** 1989. Initial stages of influenza hemagglutinin-induced cell fusion monitored simultaneously by two fluorescent events: cytoplasmic continuity and lipid mixing. J. Cell Biol. **109:**113–122.
26. **Scheiffele, P., A. Rietveld, T. Wilk, and K. Simons.** 1999. Influenza viruses select ordered lipid domains during budding from the plasma membrane. J. Biol. Chem. **274:**2038–2044.
27. **Siegel, D. P.** 1993. Modeling protein-induced fusion: insights from the relative stability of lipidic structures, p. 475–512. *In* J. Bentz (ed.), Viral fusion mechanisms. CRC Press, Boca Raton, Fla.
28. **Simons, K., and E. Ikonen.** 1997. Functional rafts in cell membranes. Nature **387:**569–572.
29. **Steck, T. L., and J. A. Kant.** 1974. Preparation of impermeable ghosts and inside-out vesicles from human erythrocyte membranes. Methods Enzymol. **31:**172–180.
30. **Stegmann, T.** 1993. Influenza hemagglutinin-mediated membrane fusion does not involve inverted phase lipid intermediates. J. Biol. Chem. **268:**1716–1722.
31. **Stegmann, T., I. Bartoldus, and J. Zumbrunn.** 1995. Influenza hemagglutinin-mediated membrane fusion: influence of receptor binding on the lag phase preceding fusion. Biochemistry **34:**1825–1832.
32. **Stegmann, T., F. P. Booy, and J. Wilschut.** 1987. Effects of low pH on influenza virus. Activation and inactivation of the membrane fusion capacity of the hemagglutinin. J. Biol. Chem. **262:**17744–17749.
33. **Stegmann, T., and A. Helenius.** 1993. Influenza virus fusion: from models toward a mechanism, p. 89–111. *In* J. Bentz (ed.), Viral fusion mechanisms. CRC Press, Boca Raton, Fla.
34. **Stegmann, T., D. Hoekstra, G. Scherphof, and J. Wilschut.** 1986. Fusion activity of influenza virus: a comparison between biological and artificial target membrane vesicles. J. Biol. Chem. **261:**10966–10969.
35. **Stegmann, T., H. W. Morselt, F. P. Booy, J. F. van Breemen, G. Scherphof, and J. Wilschut.** 1987. Functional reconstitution of influenza virus envelopes. EMBO J. **6:**2651–2659.
36. **Stegmann, T., J. M. White, and A. Helenius.** 1990. Intermediates in influenza induced membrane fusion. EMBO J. **9:**4231–4241.
37. **Struck, D. K., D. Hoekstra, and R. E. Pagano.** 1981. Use of resonance energy transfer to monitor membrane fusion. Biochemistry **20:**4093–4099.
38. **Weber, T., G. Paesold, C. Galli, R. Mischler, G. Semenza, and J. Brunner.** 1994. Evidence of H^+-induced insertion of influenza hemagglutinin HA2 N-terminal segment into the viral membrane. J. Biol. Chem. **18535–18538.**
39. **Wilschut, J., and R. Bron.** 1993. The influenza virus hemagglutinin: membrane fusion activity in intact virions and reconstituted virosomes, p. 133–161. *In* J. Bentz (ed.), Viral fusion mechanisms. CRC Press, Boca Raton, Fla.
40. **Wilson, I. A., J. J. Skehel, and D. C. Wiley.** 1981. Structure of the haemagglutinin membrane glycoprotein of influenza virus at 3 Å resolution. Nature **289:**366–375.